Electronic Supplementary Material (ESI) for Physical Chemistry Chemical Physics.

Supplementary Information: **Confinement-Induced Clustering of H_2 and CO_2 Gas Molecules in Hydrated Nanopores**

Aditya Choudhary and Tuan A. Ho*

Geochemistry Department, Sandia National Laboratories, Albuquerque, NM 87185, USA

**Corresponding author: taho@sandia.gov*

1. Simulation setups and details for systems in Figure 1 and Figure 2 in the main text

The bulk-water system in Figure 1a of main manuscript has the dimension of $42.0\ \text{Å} \times 42.0\ \text{Å} \times 42.0\text{Å}$, that contains 1690 water molecules. For pyrophyllite systems in Figure 1b and c in the main text and in Figure S1a, the sizes of the simulation box along x and z directions are 41.28 Å and 35.864 Å, respectively. While the sizes of box along y-axis, perpendicular to the surface, is 16.26 Å, and 13.26 Å for 2W and 1W, respectively. There are 320 water molecules in 2W system and 180 water molecules in 1W system. For gibbsite (Figure 2a, 2b and Figure S1b), the sizes of box along x and z directions are 43.86 Å and 36.02 Å, respectively. While the sizes of box along y-axis are 15.69 Å and 12.48 Å for 2W and 1W, respectively. There are 320 water molecules in 2W system and 180 water molecules in 1W system. In each of the mentioned systems, there are two CO_2 or two H_2 molecules.

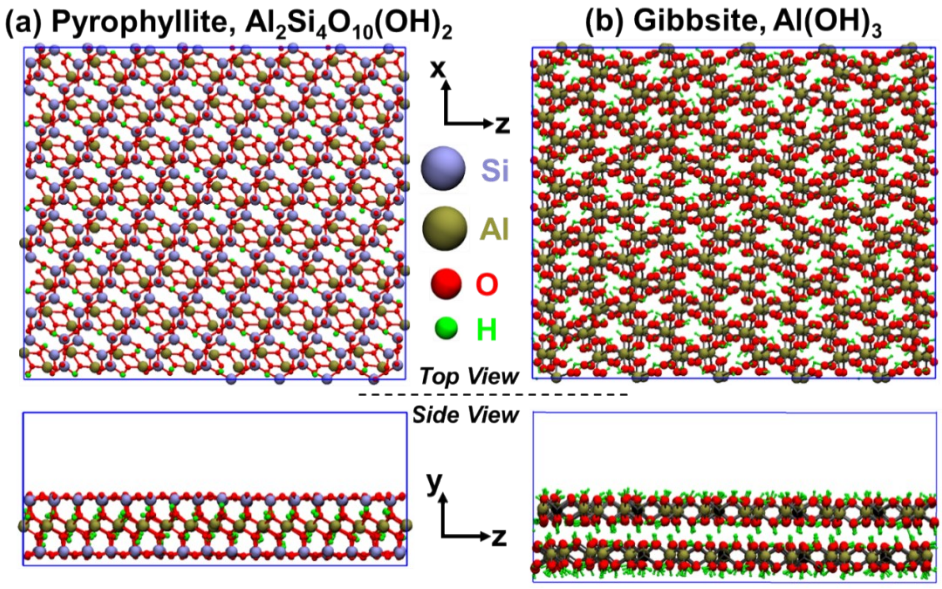

Figure S1. Top and side views of (a) pyrophyllite and (b) gibbsite interlayers. Water molecules are not shown in the snapshots.

Molecular dynamics (MD) simulations are performed with timestep of 1 fs at 300K and 1 atm, which is controlled through Nosé–Hoover thermostat and barostat.[1, 2] The description of force field parameters is provided in main manuscript. During the course of simulations, both CO_2 and H_2 are molecules are considered as a rigid body (using "fix rigid" command in LAMMPS). The Lennard-Jones (LJ) potential is defined using the following function:

$$V_{LJ} = 4\varepsilon\left[\left(\frac{\sigma}{r}\right)^{12} - \left(\frac{\sigma}{r}\right)^{6}\right] \quad (1)$$

where, ε is the depth of the potential well, σ is the distance at which V_{LJ} is zero, and r is the distance between two atoms. The LJ parameters for different type of atoms are computed using arithmetic mixing rule ($\varepsilon_{ij} = \sqrt{\varepsilon_i \varepsilon_j}$; $\sigma_{ij} = 0.5 \times (\sigma_i + \sigma_j)$). The cutoff for long range electrostatic interaction is set to 10 Å. Beyond this cutoff, electrostatic interaction is resolved in reciprocal space using particle–particle particle-mesh (PPPM) method with an accuracy of 99.99%. Initial system is equilibrated using an NVT ensemble (constant number of atoms, volume, and temperature) followed by an NPT ensemble (constant number of atoms, pressure, and temperature) until the fluctuation in the simulation box size becomes insignificant. The system is then equilibrated under NVT ensemble for over 3 ns.

After that, potential of mean force (PMF) or free energy are calculated using well-tempered metadynamics (WTM) method[3] as implemented in Colvars module.[4] In the WTM method, history-dependent Gaussian potentials are deposited to allow a system to explore a complete energy landscape:

$$V^{WTM}(r,t) = \omega e^{-V(r,t)/k_B\Delta T} e^{-[r-r(t)]^2/2\sigma^2} \quad (2)$$

$$V(r,t) = \omega e^{-[r-r(t)]^2/2\sigma^2} \quad (3)$$

where $V(r,t)$ is the Gaussian potential in the standard metadynamics method with ω and σ are the height and width, respectively. The Gaussian potential is deposited at a fixed time interval (τ). The mean value of collective variable is r, while the instantaneous value of collective variable at time t is $r(t)$. Contrast to standard method, WTM has the Gaussian height of $\omega e^{-V(r,t)/k_B\Delta T}$, which provides ΔT as a controllable parameter that decreases the height with simulation time. Inclusion of this parameter improves the convergence. For all the systems, the value of ω, σ, τ, and ΔT are 1.0 kcal/mol, 0.2 Å, 100 fs, and 500 K, respectively. The convergence of free energy profiles (Figure 1 and Figure 2) for pyrophyllite and gibbsite systems are given in Figure S2 and Figure S3, respectively. In addition, we also perform PMF calculation for two CO_2 or two H_2 molecules in vacuum, and the result is reported in Figure S4.

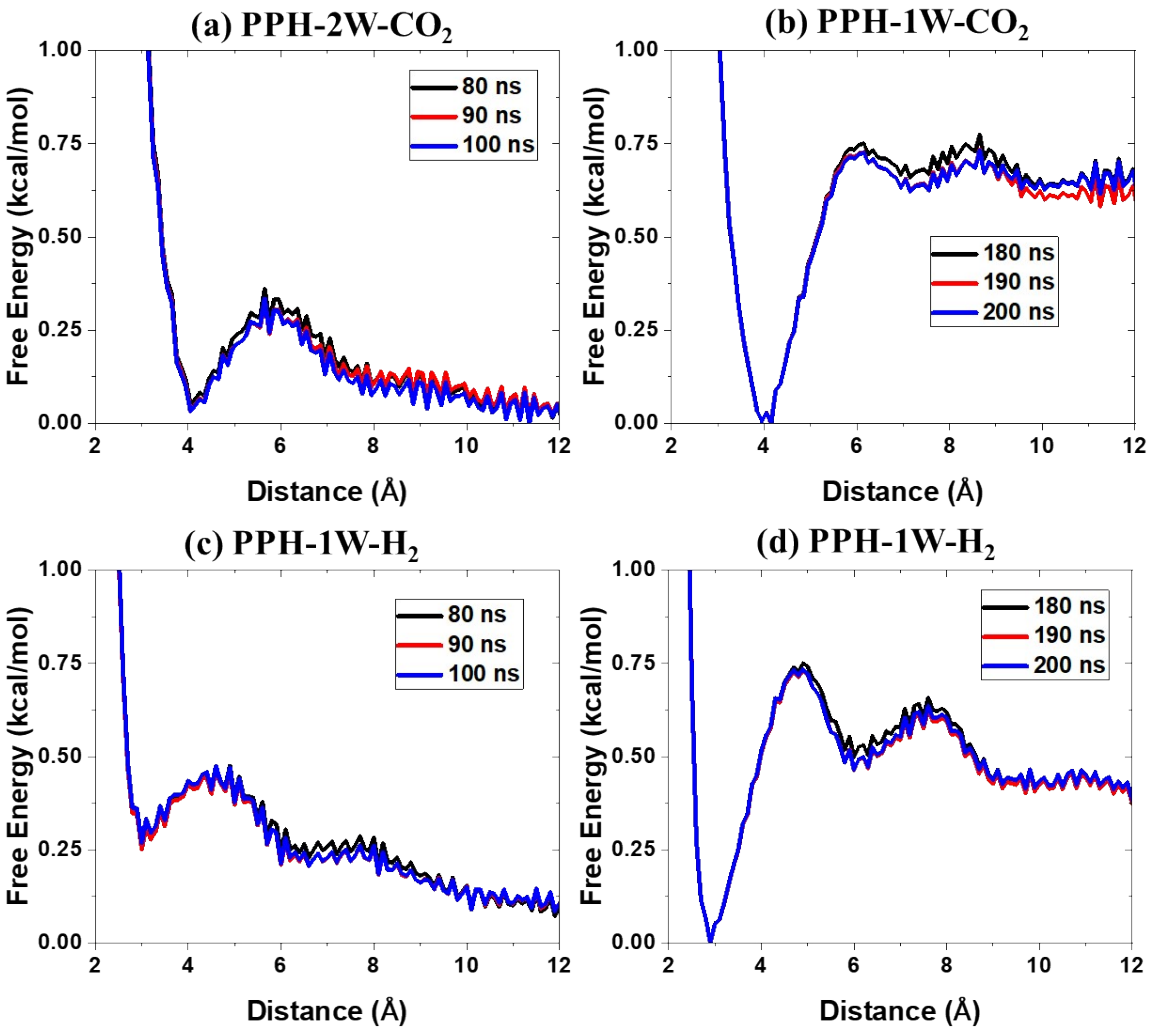

Figure S2. The free energy profiles, at different simulation times, as a function of distance between two CO_2 molecules in (a) 2W pyrophyllite, (b) 1W pyrophyllite, and two H_2 molecules in (c) 2W pyrophyllite, (d) 1W pyrophyllite interlayers.

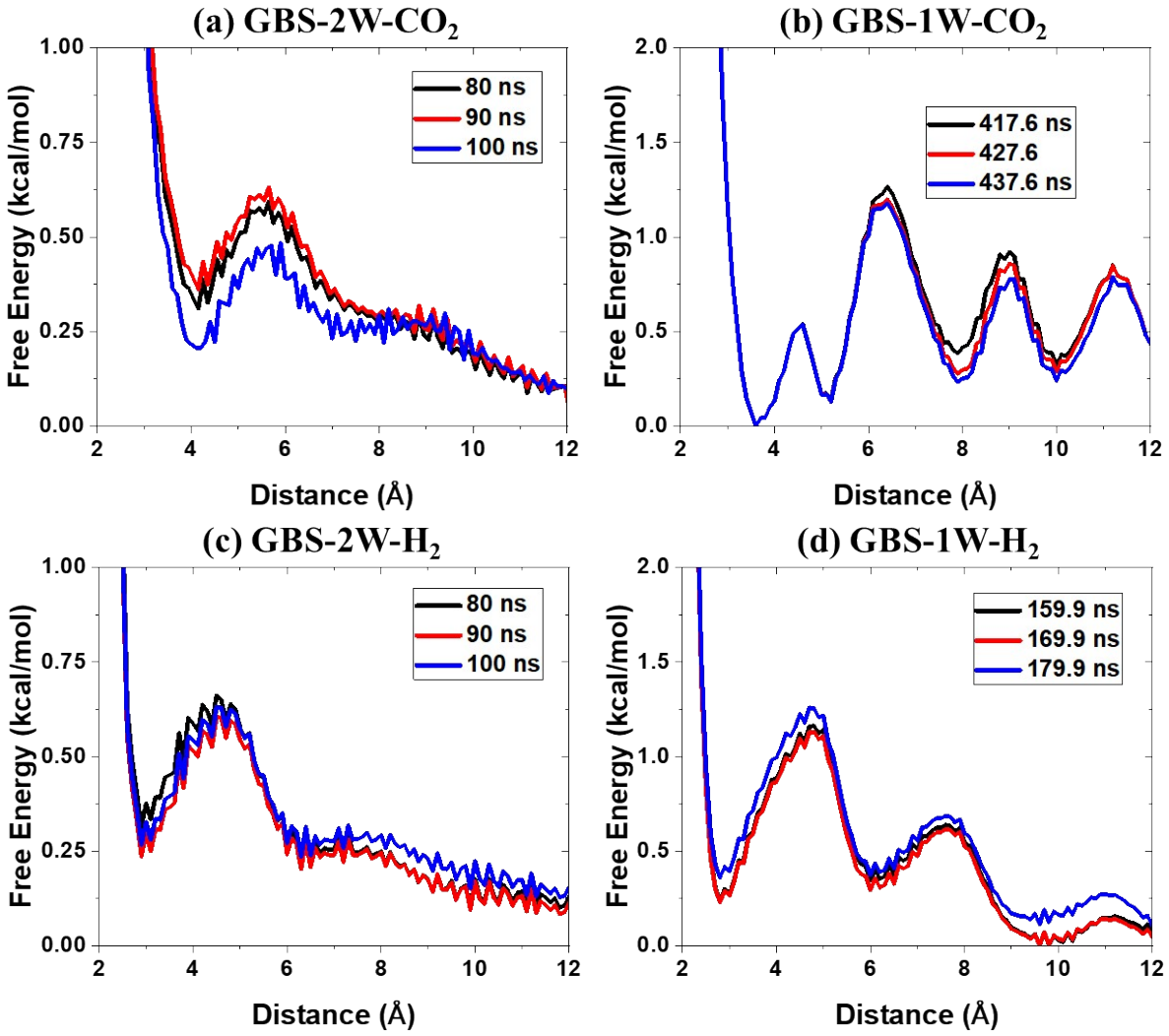

Figure S3. The free energy profiles, at different simulation times, as a function of distance between two CO_2 molecules in (a) 2W gibbsite, (b) 1W gibbsite, and two H_2 molecules in (c) 2W gibbsite, (d) 1W gibbsite interlayers.

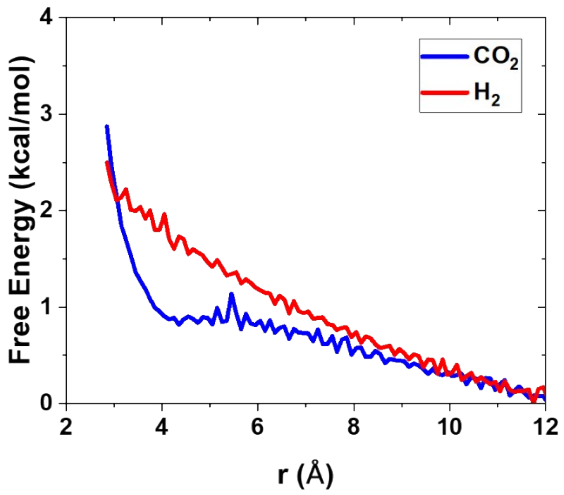

Figure S4. The free energy as a function of distance between two CO_2 and H_2 molecules in vacuum.

2. System setups and details for the results in Figure 3 in the main text.

In order to quantify the probability of finding a gas molecule in a given cluster, we simulate pyrophyllite (Figure S5) and gibbsite hydrated interlayers with 10 CO_2/H_2 gas molecules. The simulation systems are anolog to those used in Figure 1 and Figure 2. However, in Figure 1 and 2, there are just two gas molecules. Here, we have added 8 extra gas molecules solvated in 8 fewer water molecules. The box sizes in all the dimensions are kept the same as in Figure 1 and 2. All simulations are run at 300 K and 1 atm with timestep of 1 fs. Systems are equilibrated in an NVT ensemble for at least 3 ns followed by production runs of over 16 ns.

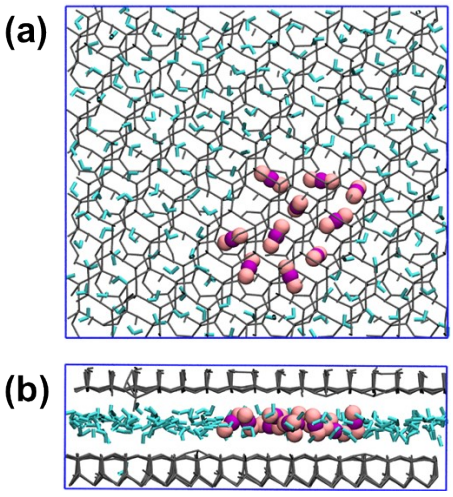

Figure S5. (a) Top and (b) side views of 1W pyrophyllite interlayer with 10 CO_2 molecules. The grey color denotes pyrophyllite, cyan color indicates water, and CO_2 molecules are represented by purple and pink spheres.

3. Simulation setups and details for the results in Figure 4.

The simulation models reported in Figure 4 a, b have edges which are different from the models used in Figures 1, 2, and 3. A detailed procedure for constructing the pyrophyllite layers with edges (Figure S6) is provided elsewhere.[5] Briefly, we began by cleaving a pyrophyllite layer on its (0 1 0) face,[6] addressing the resulting broken bonds by introducing -OH groups or -H atoms. This was done to ensure that every silicon atom at the edge forms coordinates with four oxygen atoms and each edge aluminum atom coordinates five oxygen atoms. In an aqueous solution, a five-coordinated aluminum atom at the edge forms an additional bond with a water molecule to achieve its six-coordinated state.[7] For gibbsite, we create a gibbsite layer with edge by cleaving along the (1 0 0) face, similar to the approach we used to create gibbsite particle in previous work.[8] The resultant structure has edges with 5-coordinated aluminum. A water molecule will coordinate with an edge aluminum atom to form six-coordinated configuration.

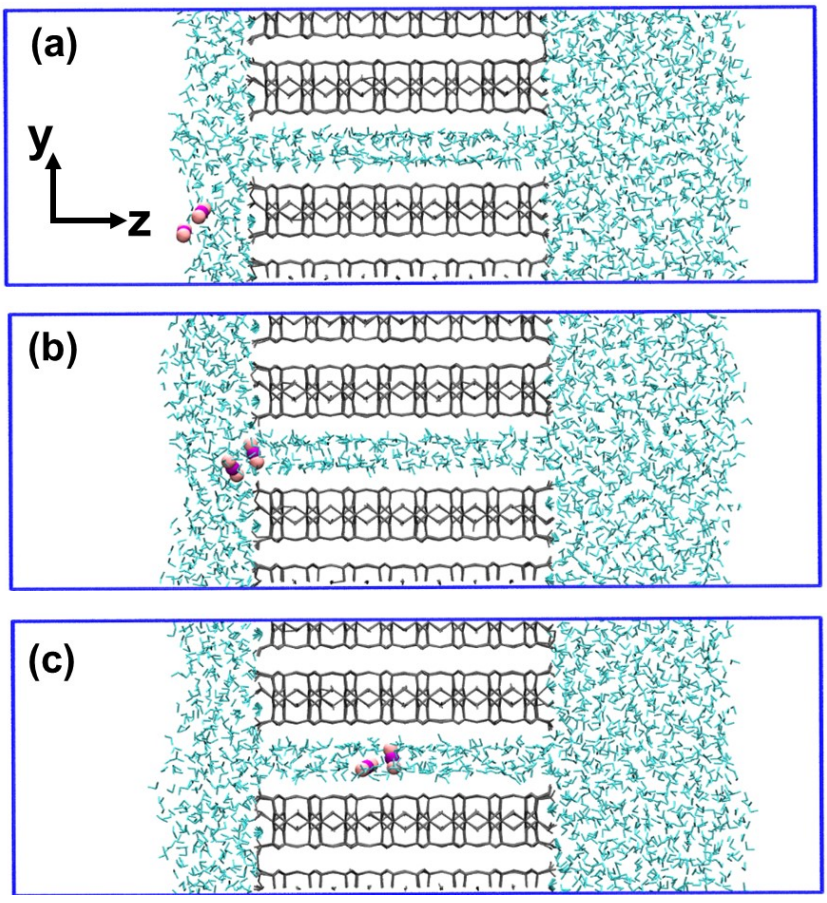

Figure S6. Simulation snapshots showing different stages of intercalation process. Location of CO_2 dimer (a) at the air/water interface, (b) at the pore opening of pyrophyllite, and (c) inside the 2W interlayer of pyrophyllite.

The formed pyrophyllite/gibbsite layers with edges then immersed in water as shown in Figure S6. Note, the empty space in the simulation box denotes the vacuum. For pyrophyllite, the size of the box along x, y, and z directions are 31.0602 Å, 34 Å, and 100 Å, respectively. Whereas for gibbsite, the size of the box along x, y, and z directions are 20.312 Å, 34.9818 Å, and 110 Å, respectively. The pyrophyllite is 36 Å long in z direction, and the gibbsite is 35.5 long in z direction. When applying periodic boundary conditions in all directions, the pyrophyllite and gibbsite structures are infinitely long in x direction. The number of water molecules in pyrophyllite and gibbsite systems are 1458 and 1260, respectively. These systems are equilibrated using NVT simulations for over 3ns. Following equilibration, well-tempered metadynamic (WTM) simulations are conducted to compute the free energy corresponding to the intercalation of CO_2 and H_2 gas from vacuum to hydrated interlayers (Figure 4c-4f). The snapshots corresponding to location '1', '2', and '3' labelled in Figure 4a are provided in Figure S6a-S6c. The value of WTM parameters, namely, ω, σ, τ, and ΔT are 1.0 kcal/mol, 0.2 Å, 100 fs, and 500 K, respectively, for pyrophyllite. The value of ω, σ, τ, and ΔT are 1.0 kcal/mol, 0.2 Å, 100 fs, and 1000 K, respectively, for gibbsite. The convergence of PMF profiles are given in Figure S7 and Figure S8.

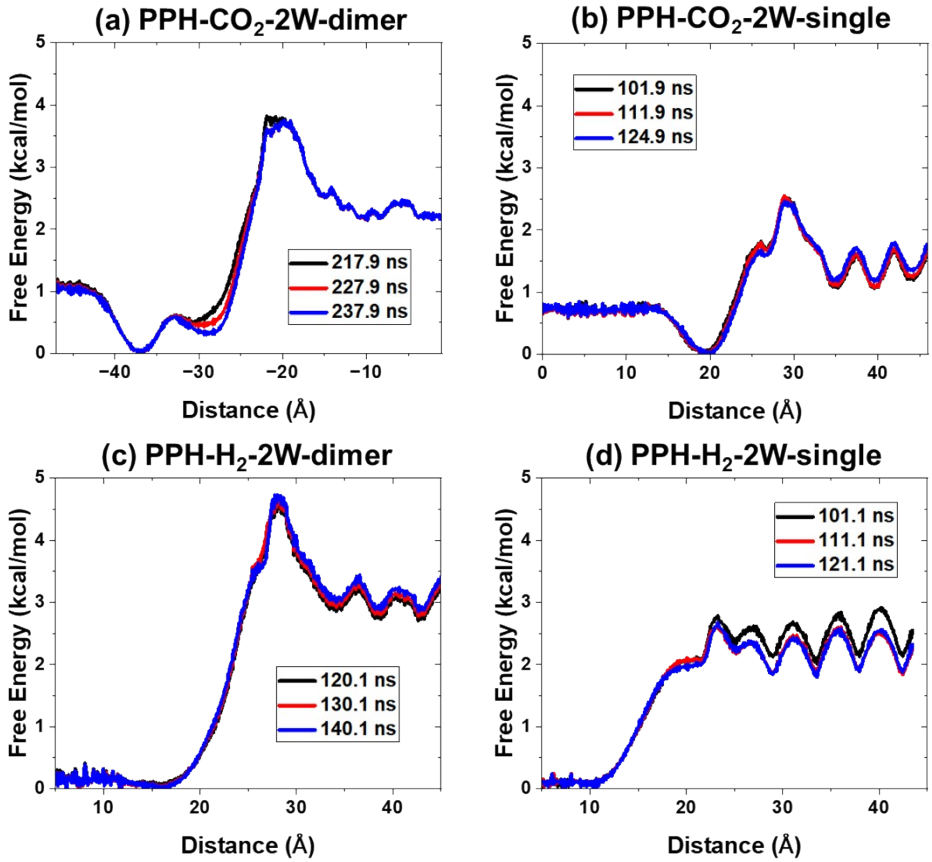

Figure S7. The free energy profiles, at different simulation times, of the intercalation of (a) CO_2 dimer, (b) CO_2 single molecule, (c) H_2 dimer, and (d) H_2 single molecule into 2W hydrated pyrophyllite interlayer. The distance in these plots is the distance of the center-of-mass of individual molecule or dimer from the vacuum phase along z-direction, where r=0 corresponds to single/dimer molecules in vacuum phase.

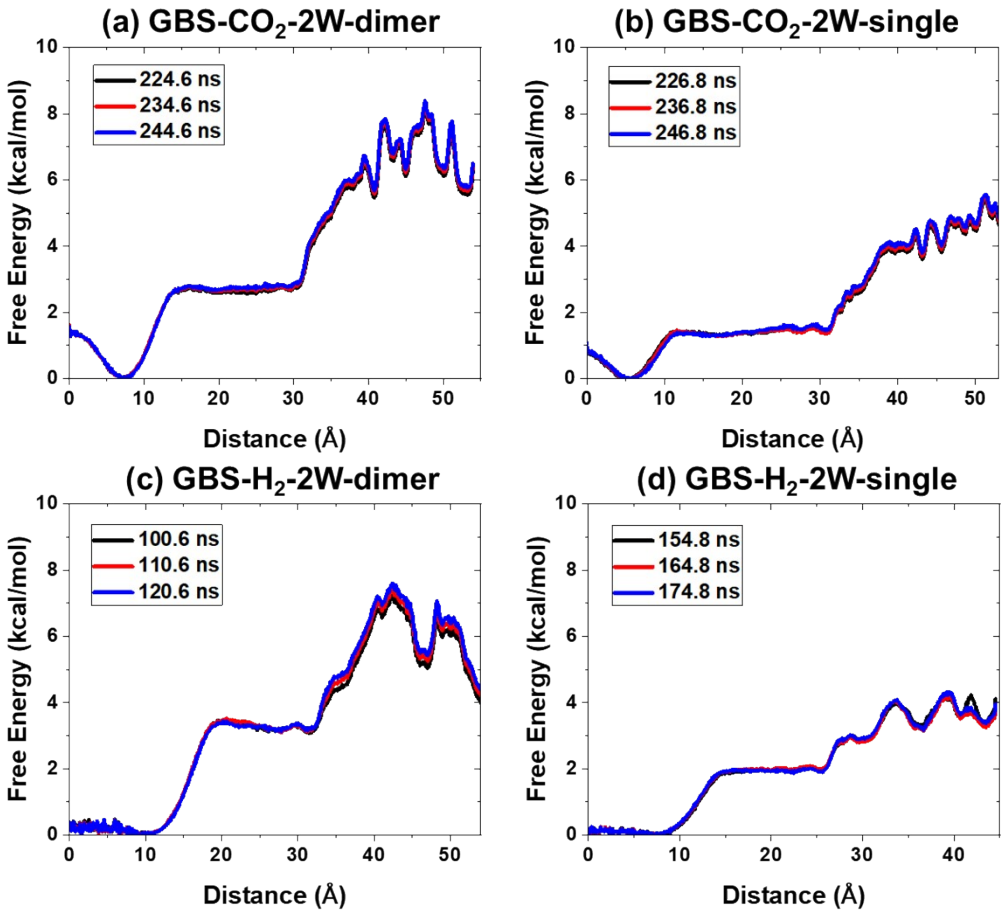

Figure S8. The free energy profiles, at different simulation times, of the intercalation of (a) CO_2 dimer, (b) CO_2 single molecule, (c) H_2 dimer, and (d) H_2 single molecule into 2W hydrated gibbsite interlayer. The distance in these plots is the distance of the center-of-mass of individual molecule or dimer from the vacuum phase along z-direction, where r=0 corresponds to single/dimer molecules in vacuum phase.

References

(1) Evans, D. J.; Holian, B. L. The Nose–Hoover thermostat. *The Journal of Chemical Physics* **1985**, *83* (8), 4069-4074. DOI: 10.1063/1.449071 (acccessed 10/18/2023).
(2) Hoover, W. G. Canonical dynamics: Equilibrium phase-space distributions. *Physical Review A* **1985**, *31* (3), 1695-1697. DOI: 10.1103/PhysRevA.31.1695.
(3) Barducci, A.; Bussi, G.; Parrinello, M. Well-Tempered Metadynamics: A Smoothly Converging and Tunable Free-Energy Method. *Physical Review Letters* **2008**, *100* (2), 020603. DOI: 10.1103/PhysRevLett.100.020603.

(4) Fiorin, G.; Klein, M. L.; Hénin, J. Using collective variables to drive molecular dynamics simulations. *Molecular Physics* **2013**, *111* (22-23), 3345-3362. DOI: 10.1080/00268976.2013.813594.
(5) Ho, T. A.; Criscenti, L. J.; Greathouse, J. A. Revealing Transition States during the Hydration of Clay Minerals. *The Journal of Physical Chemistry Letters* **2019**, *10* (13), 3704-3709. DOI: 10.1021/acs.jpclett.9b01565.
(6) Harvey, J. A.; Johnston, C. T.; Criscenti, L. J.; Greathouse, J. A. Distinguishing between bulk and edge hydroxyl vibrational properties of 2 : 1 phyllosilicates via deuteration. *Chemical Communications* **2019**, *55* (24), 3453-3456, 10.1039/C9CC00164F. DOI: 10.1039/C9CC00164F.
(7) Ho, T. A.; Greathouse, J. A.; Lee, A. S.; Criscenti, L. J. Enhanced Ion Adsorption on Mineral Nanoparticles. *Langmuir* **2018**, *34* (20), 5926-5934. DOI: 10.1021/acs.langmuir.8b00680.
(8) Ho, T. A.; Greathouse, J. A.; Wang, Y.; Criscenti, L. J. Atomistic Structure of Mineral Nano-aggregates from Simulated Compaction and Dewatering. *Scientific Reports* **2017**, *7* (1), 15286. DOI: 10.1038/s41598-017-15639-4.